Phase-retrieval algorithm for the characterization of broadband single attosecond pulses

Xi Zhao, Hui Wei, Yan Wu, and C. D. Lin

A new phase retrieval algorithm for characterization of broadband single attosecond pulses

Xi Zhao[1,2], Hui Wei[1], Yan Wu[1,3], and C. D. Lin[1*]

[1] *Department of Physics, Kansas State University, Manhattan, KS 66506, USA*
[2] *Laser Fusion Research Center, China Academy of Engineering Physics,*
Mianyang, Sichuan 621900, People's Republic of China
[3] *School of Science, Zhejiang Sci-Tech University, Hangzhou 310018, People's Republic of China*
(Dated: March 17, 2017)

Recent progress in high-order harmonic generation with few-cycle mid-infrared wavelength lasers has pushed light pulses into the water window region and beyond. These pulses have the bandwidth to support single attosecond pulses down to a few tens of attoseconds. However, the present available techniques for attosecond pulse measurement are not applicable to such pulses. Here we report a phase-retrieval method using the standard photoelectron streaking technique where an attosecond pulse is converted into its electron replica through photoionization of atoms in the presence of a time-delayed infrared laser. The iterative algorithm allows accurate reconstruction of the spectral phase of light pulses, from the extreme-ultraviolet (XUV) to soft X-rays, with pulse durations from hundreds down to a few tens of attoseconds. At the same time, the streaking laser fields, including short pulses that span a few octaves, can also be accurately retrieved. Such well-characterized single attosecond pulses in the XUV to the soft X-ray region are required for time-resolved probing of inner-shell electronic dynamics of matter at their own timescale of a few tens of attoseconds.

PACS numbers: 32.80.Fb, 42.65.Re

I. INTRODUCTION

In the last decade and half, significant attention has been devoted to the development of attosecond science and technology, in particular, the generation of attosecond pulses and how they can be used to probe dynamics of electrons at the ever-shorter timescale, for atoms, molecules and nanostructure materials[1]. Various techniques have been developed to generate broadband extreme ultraviolet (XUV) light that has available continuum bandwidth capable of supporting pulse duration of a few tens to hundreds of attoseconds, such as amplitude gating[2], ionization gating[3], polarization gating[5], double optical gating[4], and wavefront rotation method[6]. Similarly, using few-cycle phase-stabilized mid-infrared wavelength lasers, ultra-broadband super-continuum harmonics up to the water-window and beyond have been reported[7–15]. If these pulses are transform-limited, the resulting durations of the attosecond pulses are expected to range from 30 attoseconds down to even a few attoseconds. However, it is well known that high-order harmonics generated in a gas medium exhibit attochirps[16]. Over the broadband, the chirp can be quite significant if the phase has not been compensated[17]. Clearly, full temporal characterization of these pulses is needed. Unfortunately, it cannot be carried out with the current pulse measurement techniques.

Attosecond pulses with durations of 67 as[18] or 80 as[2] have been reported using typical 800 nm driving lasers. These pulses are characterized based on the principle of attosecond streaking where the XUV's electric field is converted to an electron spectrum, or spectrogram, through photoelectron emission in atoms, in the presence of a moderately intense IR laser field. In the streaking spectrogram, the momentum of the electron is shifted by an amount depending on the relative time delay between the XUV and the IR pulses. Thus time information of the attosecond pulse is encoded in the amount of momentum shift in the streaked spectrogram. A standard technique known as FROG-CRAB (Frequency-Resolved Optical Gating for Complete Reconstruction of Attosecond Bursts)[19–21] has been used to retrieve the attosecond pulse, which stems from the FROG (Frequency-Resolved Optical Gating) method for the characterization of femtosecond infrared laser pulses. The retrieval is based on an iterative process by matching the measured photoelectron spectrogram to a FROG-CRAB trace from an unknown XUV pulse and an unknown IR field.

The FROG-CRAB has employed a number of approximations. The most damaging one is the so-called "central momentum approximation", which limits its applicability only to narrow bandwidth pulses, i.e., the approximation is reasonable only when the bandwidth of the attosecond pulse is much smaller than the central energy of the photoelectron. This approximation is required in order to be able to adopt the existing inversion algorithm used in FROG, which was widely used for femtosecond laser pulse characterization. The failure of FROG-CRAB for retrieving broadband attosecond pulses is well-known. An earlier PROOF method (Phase Retrieval by Omega Oscillation Filtering) was proposed for such pulses[26]. However, the method relies on a relatively long and weak

*cdlin@phys.ksu.edu

streaking IR pulse, and that the dipole moment within the bandwidth is assumed to be constant. These approximations, as addressed in Wei *et al.*[27], are not consistent with broadband pulses that span many tens to hundreds of electron volts. Very recently, it has come to our attention that a method called "Volkov transform" generalized projections algorithm (VTGPA) has been proposed to retrieve broadband XUV attosecond pulses in the IR streaking field[28], but the VTGPA has not been extensively tested yet, and has not been applied to soft X-ray attosecond pulses, nor to mid-infrared streaking lasers.

In this article, we report an iterative retrieval algorithm without employing the central momentum approximation. Iterative procedure is still employed, but for efficient convergence, efforts were made to reduce the number of unknown parameters in the guessed electric fields of the XUV and the IR. We would take advantage of pulse parameters that can be measured from other experiments, for example, the spectral amplitude of the XUV pulse which in general can be obtained from photoionization measurement by the XUV alone. The IR phase and/or amplitude can be assumed to be known or unknown depending on the nature of the measurement. We chose to expand the unknown amplitude and/or phase of the XUV and the IR fields in terms of the so-called B-spline basis functions[22]. Such expansions are commonly used in representing a smooth function with minimum number of unknowns. We call our method phase retrieval of broadband pulses (PROBP), since the method not only can retrieve broadband single attosecond pulses in the XUV or soft X-rays, but also can retrieve wideband infrared streaking fields spanning over a few octaves that are used to generate supercontinuum harmonics[23–25]. In Section II we briefly introduce the PROBP method, including the strong field approximation (SFA) on which this method is based, and the way to construct unknown functions using B-spline basis. In Section III we simulate the photoelectron spectrograms in various experimental conditions, and then test the accuracy of the PROBP method in retrieving the single attosecond pulse as well as the steaking IR field. Finally we summarize this article in Section IV. Atomic units are used unless noted otherwise.

II. PRINCIPLE OF PROBP

A. Strong field approximation

Both the FROG-CRAB, VTGPA and PROBP methods assume that the measured photoelectron spectrogram can be modeled by SFA[19, 20]:

$$
\begin{aligned}
S(p,\tau) = & \left| \int_{-\infty}^{\infty} E_{XUV}(t-\tau)d(p+A(t)) \right. \\
& \left. \times e^{-i\Phi(p,t)} e^{i\left(\frac{p^2}{2}+I_P\right)t} dt \right|^2,
\end{aligned}
\tag{1}
$$

where $E_{XUV}(t)$ is the XUV or the soft X-ray field to be characterized. For simplicity we use XUV to include soft X-rays, and IR to include Mid-IR in the following unless otherwise specified. τ is the time delay between XUV and IR, $d(p)$ is the transition dipole between the initial bound state and final continuum state of the atom. The vector potential of the IR is $A(t) = -\int_{-\infty}^{t} E_{IR}(t')dt'$ and the phase function $\Phi(p,t)$ reads

$$
\Phi(p,t) = \int_{t}^{\infty} \left[pA(t') + \frac{A^2(t')}{2} \right] dt'.
\tag{2}
$$

The polarization directions of the XUV, the IR and the direction of the photoelectrons are all taken along the z-axis. In the FROG-CRAB method, a central momentum approximation was imposed on Eqs. (1) and (2), where $\Phi(p,t)$ is replaced by $\Phi(p_0,t)$, and p_0 is the central momentum of the photoelectrons. In PROBP (and in VTGPA) no such approximation is imposed.

In our method, the XUV pulse in the energy domain is expressed as

$$
E_{XUV}(\Omega) = U(\Omega)e^{-i\phi_{XUV}(\Omega)}.
\tag{3}
$$

A single color, multi-cycle IR field in the time domain is expressed as

$$
E_{IR}(t) = f(t)\cos\left(\omega_L t + \varphi_{IR}(t)\right),
\tag{4}
$$

while a broadband IR pulse consisting of multiple colors is better represented in the frequency domain

$$
E_{IR}(\omega) = A(\omega)e^{-i\phi_{IR}(\omega)}.
\tag{5}
$$

In this work, we assume that the amplitude and phase of the transition dipole $d(p)$ is known. In our simulations Ne is chosen as the target, modeled by a single-electron model potential[31]. Therefore the transition dipole $d(p)$ can be calculated accurately. We always use IR peak intensity at 10^{13} W/cm^2 and XUV at 10^{12} W/cm^2. The actual intensity of the latter is not important since the XUV enters Eq. (1) linearly. We also assume that the spectral amplitude of the XUV, i.e., $U(\Omega)$ is known since it can be extracted from XUV photoionization experiment without the IR.

B. Expanding unknown functions using B-spline

In the simulations, the "experimental" spectrogram is obtained with known input XUV and IR fields. Our goal is to retrieve the phase of the XUV, i.e., $\phi_{XUV}(\Omega)$ as well as the IR field as if they were unknown. The IR field can be retrieved either in the time domain with unknown functions $f(t)$ and $\varphi_{IR}(t)$, or in the frequency domain with unknown functions $A(\omega)$ and $\phi_{IR}(\omega)$. Therefore there are three unknown functions in total. Each unknown function is expanded in terms of B-spline basis functions.

In general, a smooth function $f(x)$ can be expanded as

$$f(x) = \sum_{i=1}^{n} g_i B_i^k(x), \qquad (6)$$

where g_i are expansion coefficients. i is the index of the B-Spline function. The k_{th} order B-Spline functions $B_i^k(x)$ are defined through

$$B_i^1(x) = \begin{cases} 1 & x_i \leq x \leq x_{i+1} \\ 0 & \text{otherwise} \end{cases} \qquad (7)$$

$$B_i^k(x) = \frac{x - x_i}{x_{i+k-1} - x_i} B_i^{k-1}(x) + \frac{x_{i+k} - x}{x_{i+k} - x_{i+1}} B_{i+1}^{k-1}(x). \qquad (8)$$

Here $\{x_i\}$ are the knot points. If there are n B-Spline basis functions of the order k, the total number of knot points is $n+k$. B-Spline function is a powerful tool for fitting a smooth function[22], and it has been widely used in computational physics. Figure 1 shows an example where the input smooth function is accurately reconstructed by seven B-spline basis functions, by optimizing the knot points and the expansion coefficients. The red solid line is the function to be fitted while the black dash line corresponds to the reconstructed function. The typical B-Spline basis functions are also shown in the graph.
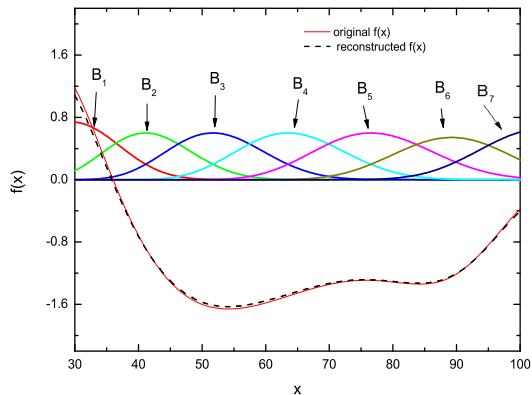

FIG. 1: (Color online) Illustration of expanding a smooth function in terms of B-spline basis functions. The input function (red solid line) is compared with the reconstructed one (black dashed line). Seven B-Spline functions with the order of five are used in the reconstruction.

In our situation, we define the guessed B-spline expansion coefficients for the three unknown functions as $\{a_i\}$, $\{b_i\}$ and $\{c_i\}$, respectively. From these coefficients the guessed XUV and IR fields can be constructed, and then for each discrete set of points $\{E_k, \tau_l\}$, the corresponding spectrogram is obtained by using Eq. (1). Typically we chose 100 to 500 points in time delay and 100 points in energy. The error function is defined as

$$E[a_i, b_i, c_i] = \sum_{k,l} (S_0(E_k, \tau_l) - S_1(E_k, \tau_l))^2, \qquad (9)$$

where S_0 and S_1 are the input and reconstructed spectrograms respectively. We use the genetic algorithm (GA) to find the optimal parameters $\{a_i, b_i, c_i\}$ that would minimize Eq. (9). The GA runs a large number of generations (typically 50,000 to 100,000 generations) until convergence is achieved. The optimal parameters $\{a_i, b_i, c_i\}$ are then used to reconstruct the XUV and IR pulses.

The convergence of the retrieval algorithm depends on how we choose the number n and the order k of B-Spline basis and how we place the knot points $\{x_i\}$ for each unknown function. If we know the spectral amplitude of the XUV pulse, for example, see Fig. 2(b), then in order to retrieve the spectral phase of the XUV, more knot points can be placed within the spectral range of the XUV and less outside, as illustrated by Fig. 2(a). Since the spectral amplitude and phase of the IR are not known, the knot points are distributed more evenly for both functions.
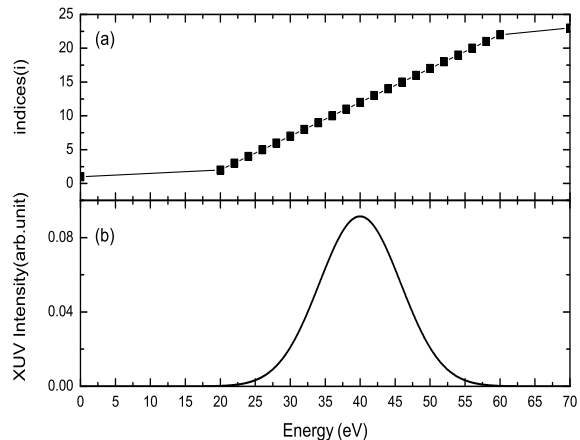

FIG. 2: (Color online) The scheme that shows how we optimize the distribution of the knot points (a) for XUV phase based on the spectral amplitude of the XUV pulse (b).

Because there are three unknown functions constructed by three sets of B-spline functions, each with its own parameters n and k, the optimization is carried out as follows. First, we search the best n_1 and k_1 by fixing a given collection of n_2, k_2, n_3, k_3. We scan all possible n_1 and k_1 in the GA and calculate the error after a few generations, for example, 100 generations. The combination n_1 and k_1 which leads to the smallest error is documented. Next we perform the same procedure to find the best n_2, k_2 by fixing n_1, k_1, n_3, k_3, in which n_1, k_1 have been optimized in the first step already. Thirdly

we find the best n_3 and k_3 using the n_1, k_1, n_2, k_2 obtained from the previous steps. The whole process can be repeated for several times. Once we find the best n_i and k_i, ($i = 1, 2, 3$), the GA converges very fast and the optimization is very efficient. In our simulations, it only takes about 30 minutes to get converged results. Below we illustrate various results from our simulations.

III. SIMULATIONS AND RESULTS

A. Equivalence of PROBP and FROG-CRAB for narrow-bandwidth attosecond pulses

In the first simulation, we consider three XUV pulses, each with central photon energy of 40 eV and spectral width of 11 eV. The spectral width is always referred to the full width at half maximum (FWHM). The IR pulse has central wavelength of 800 nm and duration of 4.4 fs. In this example the spectrogram is calculated by solving the time-dependent Schrödinger equation (TDSE), instead of using Eq. (1). This allows us to test how SFA affects the accuracy of the retrieval of the XUV phase. The three XUV pulses differ only by their spectral phases. The first one is transform-limited, with duration of 160 as. The second and third are chirped with duration of 200 and 250 as, respectively. Figure 3 documents the results of the simulation. Along the left column, the spectrograms are shown. The differences among them are quite discernable. Using the FROG-CRAB and PROBP methods the XUV phase for each pulse is retrieved (the amplitude is set to be the input one), as shown in the middle column. Clearly the phases are accurately retrieved except near the wings where the spectral amplitude is already small. Nevertheless it does show that PROBP is closer to the input phase. From the known spectral amplitude and retrieved phase, the temporal intensity of each XUV pulse is obtained, see the right column. They all agree very well with the input pulses. This example shows that Eq. (1), even though it is an approximate theory, can still be used to retrieve the XUV pulses.

B. Broadband XUV pulses where FROG-CRAB fails

For a transform-limited attosecond pulse with duration of one atomic unit, i.e., 24 as, the bandwidth is 75 eV. In this example, we consider a chirped XUV pulse with duration of 52 as, central photon energy of 80 eV and bandwidth of 90 eV. The input XUV phase is shown as the red dash line in Fig. 4(a). The SFA, Eq. (1), was used to simulate the spectrogram with the IR given in Section III A. Using FROG-CRAB, the retrieved XUV spectral phase, displayed as the blue dash-dot line in Fig. 4(a), shows significant deviation from the input phase, while the present PROBP, see the black solid line, is capable of retrieving the highly modulated spectral phase. The

reconstructed temporal profiles, as shown in Fig. 4(b), reveal that the FROG-CRAB method fails to reproduce the chirp of the input pulse. It predicts a pulse duration of 25 as, while the PROBP method recovers a pulse duration of 51 as, as compared to the input value of 52 as, as well as a good agreement of spectral phase over the whole bandwidth. This example testifies the severe failure of the central momentum approximation used in the FROG-CRAB method, and the success of the PROBP method for a broadband XUV pulse.

C. Phase retrieval of attosecond pulses in the water-window region

High-order harmonics in the "water window" with photon energy ranging from 280 to 530 eV have been reported in a number of laboratories in recent years[7–15]. Such soft X-ray harmonics are needed to excite core-level transitions in materials. They are generated by long-wavelength mid-infrared lasers using an OPA or OPCPA, pumped by a Ti-Sapphire laser. When generated with few-cycle mid-infrared lasers it has been found that the generated harmonics exhibit supercontinuum spectrum, with the possibility of supporting single attosecond pulses of durations of less than thirty down to a few attoseconds. However, due to the atto-chirp of the generated harmonics, without post phase compensation, it is fortuitous to claim single attosecond pulses with such short durations. Unfortunately, since the prevalent FROG-CRAB method is not expected to be valid for retrieving broadband attosecond pulses, pulse duration of attosecond pulses in the water-window region has not been retrieved so far.

In this example, we choose three input attosecond pulses with central energy of 300 eV and bandwidth of 46 eV. In the transform-limited case this spectrum will support a pulse duration of 46 as. The three input XUV pulses differ by their spectral phases, see Figs. 5(a), (c) and (e). We assume that the soft X-ray harmonics are generated by a four-cycle 2000-nm mid-infrared laser which is also used as the streaking field. In this example, we have not been able to obtain converged results for the spectral phase using FROG-CRAB. On the other hand, with the PROBP method, we have successfully retrieved the spectral phases for all the three cases. The resulting temporal intensity for each pulse has also been successfully retrieved, see Figs. 5(b), (d) and (f). The input pulse durations of the three examples are 436, 147 and 46 as, to be compared to the durations retrieved from PROBP, 419, 156 and 50 as, respectively.

Besides the central momentum approximation, the FROG-CRAB algorithm we used[20] relies on the discretization of the time axis. Using mid-infrared lasers as the streaking field, the phase $\Phi(p, t)$ in Eq. (2) grows like λ^2, thus the factor $e^{-i\Phi(p,t)}$ in Eq. (1) oscillates very rapidly, and it would require a very small time step dt in the integration to less than 1 as. In the FROG-CRAB algorithm, the time domain and energy domain are re-
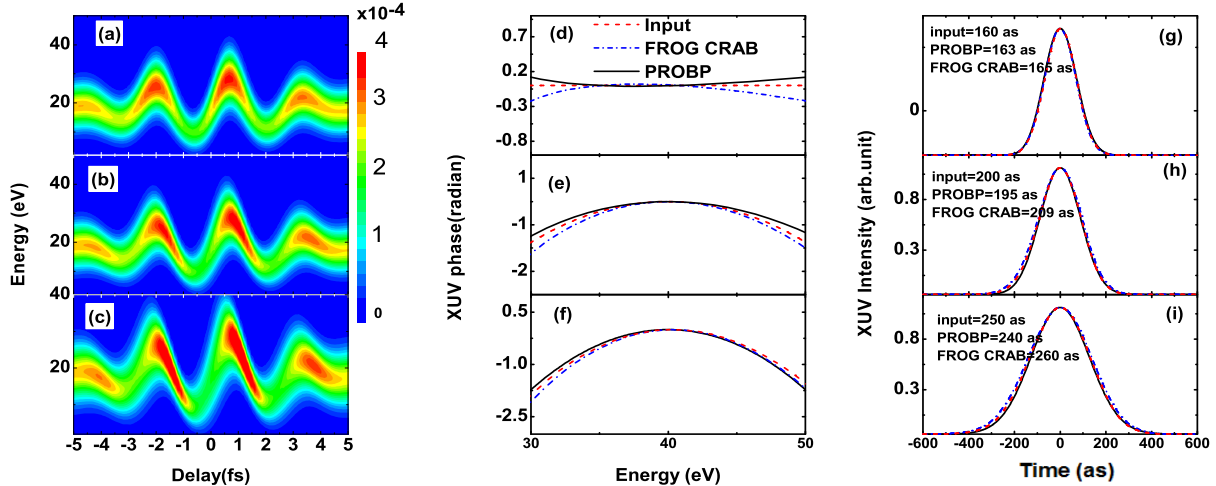
FIG. 3: (Color online) Characterization of three XUV pulses centered at 40 eV with a bandwidth of 11 eV. The FWHM durations of these pulses are 160 as, 200 as and 250 as, respectively. (a), (b) and (c) are the input spectrograms simulated by TDSE, with the three XUV pulses. (d), (e) and (f) are the spectral phases of the three XUV pulses. (g), (h) and (i) are the XUV intensity profiles in the time domain. The red dash lines are the input data, the black solid lines are retrieved from the PROBP method, while the blue dash-dot lines are retrieved from FROG-CRAB.
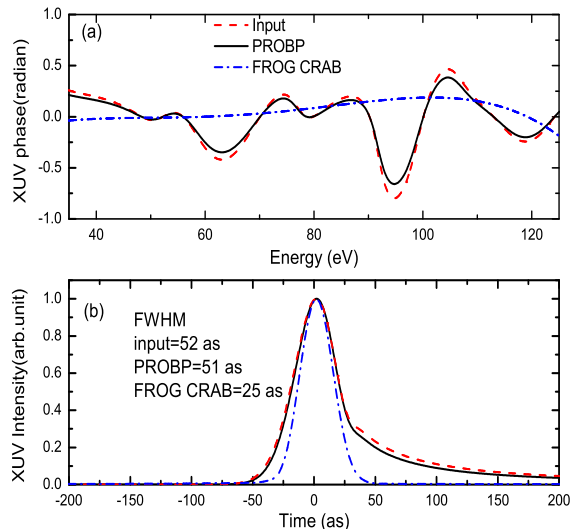

FIG. 4: (Color online) Comparison between FROG-CRAB and PROBP for characterizing an XUV pulse centered at 80 eV with a broad bandwidth of 90 eV. (a) is the XUV spectral phase. (b) is the XUV intensity profile. The red dash lines are the input data, the black solid lines are retrieved from the PROBP method, while the blue dash-dot lines are retrieved from the FROG-CRAB.

lated by the fast Fourier transform (FFT), which imposes a sampling condition $dt \times dE = 2\pi/N$. Here dE is the energy step and N is the number of data points in both time and energy domains. If we also limit the energy step dE to less than 0.1 eV, then N should be greater than 40,000. For such a large data set, it will take an unaffordable time for FROG-CRAB to get a converged result. This makes the current FROG-CRAB retrieval method not applicable for mid-infrared streaking fields, more than just retrieving incorrect results.

D. Sensitivity of the phase retrieval to noise in the spectrogram

The examples given above use the spectrogram generated directly from solving TDSE (Section III A) or calculated from the SFA (Section III B and C). When applying our method to real experimental data, there are inherent noises from the measurement. To test the sensitivity of the retrieved phase with respect to the noise, we artificially incorporate a random error up to 5% to each data point. In this test, the input parameters of the laser and the soft X-ray are the same as in Section III C. In Fig. 6, the top frames show the spectrogram with noise, versus the one without the noise. At such a level of noise, the difference between two spectrograms is not visible. The bottom frames compare the intensity profile in the time
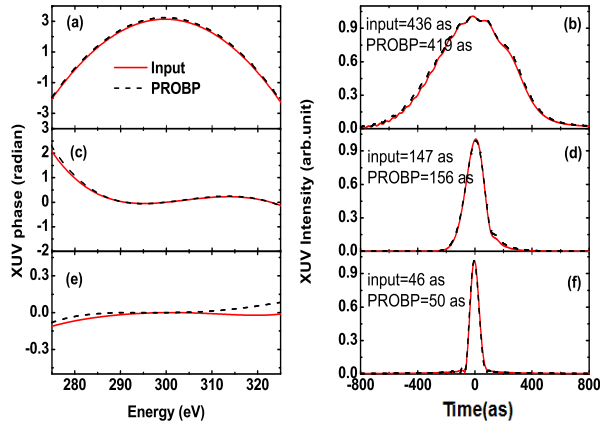
FIG. 5: (Color online) Phase retrieval of soft X-ray pulses centered at 300 eV with a bandwidth of 46 eV using PROBP. Left column: spectral phases of three different soft X-ray attosecond pulses. The spectral amplitudes for the three pulses are identical. Right column: temporal intensity of the three pulses. The red solid lines are the input data and the black dash lines are retrieved from the PROBP method. The XUV pulses are centered at 300 eV with a bandwidth of 46 eV. The wavelength of dressing mid-IR field is 2000 nm, the duration is 4 cycles.

domain and the phase in the energy domain, of the input soft X-ray pulse with respect to that retrieved using PROBP. They agree very well. Thus the retrieved results are not sensitive to the noise in the spectrogram.

E. Accurate carrier-envelope-phase retrieval of a long IR pulse

Both the FROG-CRAB and the PROBP allow the retrieval of the IR pulse as well as the XUV pulse. In this test, we examine how accurately the IR pulse is retrieved. It is well-known that for transform-limited few-cycle IR pulses, the carrier-envelope phase (CEP) will affect the nonlinear interaction of the laser pulse with matter. While the relative CEP between two few-cycle pulses can be measured from the experiment, the absolute value of the CEP is difficult to determine. If single attosecond pulses are available in the laboratory, the IR field can also be retrieved in a streaking experiment with the method of FROG-CRAB and of PROBP. To illustrate this capability, we took a long 20 fs IR laser with 800 nm in wavelength, 10^{13} W/cm^2 in intensity, and assume that it is transform-limited with a CEP φ_0=0. In the retrieval, we assume that we do not know the IR pulse is transform-limited, thus the IR is expressed in the

form of Eq. (4) where the amplitude $f(t)$ and the phase $\varphi_{IR}(t)$ are unknown functions and each is expanded by B-spline basis functions. The SFA spectrograms were generated with this IR field and three different XUV pulses centered at 60 eV with a bandwidth of 23 eV. The XUV pulses have different chirped spectral phase so that their FWHM durations are 90 as, 130 as and 230 as, respectively, compared to the 80 as transform-limited duration. Both FROG-CRAB and PROBP were applied to retrieve the IR field, and the results are plotted in Fig. 7. Clearly, the IR field is accurately retrieved using the PROBP but not by FROG-CRAB. The PROBP method reproduced a transform-limited IR field, with CEP=0, in all three cases, while the FROG-CRAB method retrieved a chirped pulse. Note that in PROBP the retrieved IR pulse is independent of the XUV pulses used as it should be. The error of the retrieved IR field by FROG-CRAB method was already noted in our previous study[29]. Such inaccuracy in the FROG-CRAB method would induce error of the retrieved atomic dipole phase, as well as the retrieved "photoionization time delay", which has been widely investigated in recent years on different targets. Unprecedented "accuracy" of the extracted "time delay" has often been quoted in these studies without accounting for the intrinsic error of the retrieval method[30].

F. Retrieving the phase of a broadband IR pulse

To generate intense single attosecond pulses, one way conceived by experimentalists is to start with a broadband IR pulse with pulse duration of about one femtosecond. Such pulses span one or two octaves and can be obtained either with waveform synthesis of multi-color few-cycle pulses[23, 24] or by the multiple-plate supercontinuum generation method[25]. Accurate characterization of such a broadband IR field is essential in order to understand how intense single attosecond pulses are generated. The photoelectron streaking method is an excellent method to characterize both the generated single attosecond pulses as well as the streaking broadband IR field.

To test the method, we use an input IR pulse as given in Fig. 8(a), as well as an attosecond pulse with central energy of 60 eV and width of 23 eV. The phase of the XUV is set to be unknown. To describe the broadband IR, we used the parametrization in the frequency domain, Eq. (5), where the spectral phase and amplitude are to be retrieved.

Using PROBP, the retrieved spectral phase and amplitude of the IR are shown in Figs. 8(b) and (c), respectively. They are in close agreement with the input ones. From the spectral amplitude, it can be seen that the broadband IR was synthesized from four waves with wavelengths of 2000, 1600, 1100 and 800 nm. The disagreement in the retrieved spectral phase at the low-energy and the high-energy wings is in the region where
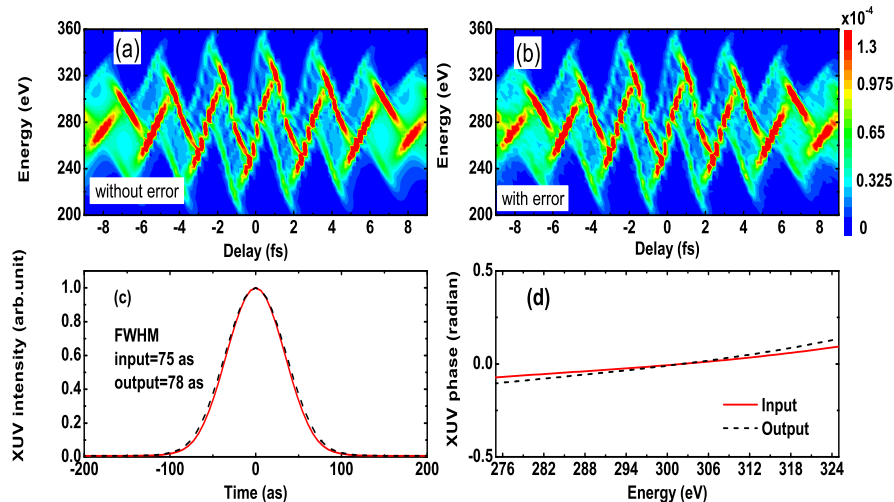
FIG. 6: (Color online) Sensitivity of the PROBP method with respect to the noise in the spectrogram. Top frames: spectrogram calculated using the SFA without any noise (left) and with a 5% random error at each point (right). Bottom frames: comparison of the soft X-ray intensity in the time domain (left), and the spectral phase in the energy domain (right), between the input pulse (red solid line) and the output one (black dash line) retrieved by the PROBP, from the spectrogram with 5% random error.
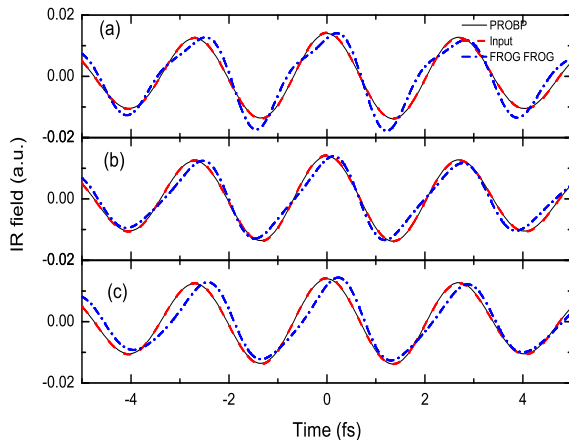

FIG. 7: (Color online) Retrieving an 800 nm, 20 fs input IR field (red dash lines) by FROG-CRAB (blue dash-dot lines) and by PROBP (black solid lines). The input IR pulse is transform-limited with CEP=0. The streaking traces were generated by using three different XUV pulses with durations of (a) 90 as, (b) 130 as and (c) 230 as, respectively. Using the PROBP method, the electric field of the IR is accurately retrieved for all three cases. The good agreement shows that the retrieved IR field is also transform-limited with the CEP=0. On the other hand, using FROG-CRAB, the retrieved IR pulses are different for the three cases and chirped.

the spectral amplitude is very small. They contribute to small errors in the retrieved electric field in the temporal domain, as shown in Fig. 8(a).

We tried the FROG-CRAB method but was unable to get converged results because the presence of mid-infrared wavelengths in the streaking field. This is similar to the failure of FROG-CRAB in Section III C. As another test, we used a waveform synthesized by four few-cycle IR pulses with wavelengths of 937, 610, 474 and 331 nm, covering almost three octaves that was used in the experiment of Refs. [23, 24]. The input pulse can be retrieved accurately by the PROBP method but not by FROG-CRAB, as demonstrated in Fig. 8(d), (e) and (f). In this example, the error of FROG-CRAB lies in the spectral amplitude of the IR. The origin of such error is due to additional approximations in the FROG-CRAB algorithm when high-frequency components are present.

IV. SUMMARY

In summary, we have demonstrated that broadband single attosecond pulses can be accurately retrieved from the streaking spectra using the retrieval algorithm PROBP. This method is applicable for characterizing soft-Xray attosecond pulses covering the water window when mid-IR dressing laser fields are used. Moreover, PROBP can retrieve the streaking IR or mid-IR field, including broadband laser pulse. In the meanwhile, this method can be applied to the typical experimental conditions that are identical to those used in the streaking measurements for narrow-band attosecond pulses where the FROG-CRAB method was used for phase retrieval.
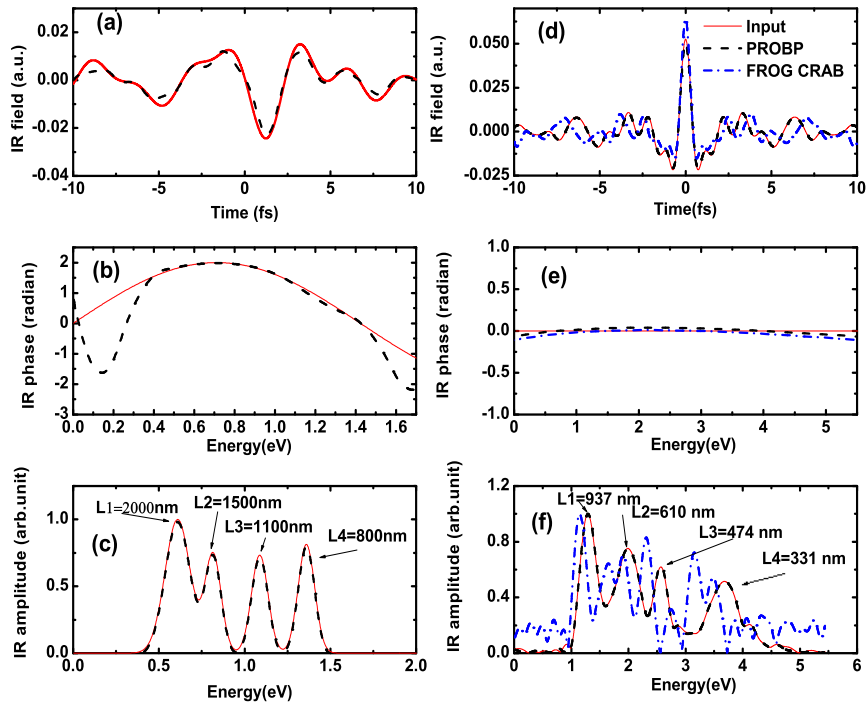
FIG. 8: (Color online) Retrieving broadband laser pulses with PROBP. (a) and (d) are the IR fields in the time domain. (b) and (f) are the IR spectral phase. (c) and (f) are the IR spectral amplitude. The red solid lines are the input field, the black dash lines are retrieved from the PROBP method and the blue dash-dot lines are retrieved from the FROG-CRAB method.

For such attosecond pulses the two methods agree reasonably well but PROBP in general is more accurate. Note that FROG-CRAB (and VTGPA) retrieve the XUV and IR fields from the time domain directly, while in PROBP we take advantage that the spectral amplitude of the XUV is readily obtained from XUV photoionization measurements. In view of the insufficient accuracy of the FROG-CRAB retrieval method in general, the precision of the retrieved parameters should always be taken with caution.

Acknowledgements

[1] F. Krausz and M. Ivanov, Rev. Mod. Phys. **81**, 163 (2009).

[2] E. Goulielmakis *et al.*, Science **320**, 1614 (2008).

[3] A. Jullien, T. Pfeifer, M. J. Abel, P. M. Nagel, M. J. Bell, D. M. Neumark, and S. R. Leone, Appl. Phys. B **93**, 433 (2008).

[4] H. Mashiko, S. Gilbertson, C. Li, S. D. Khan, M. M. Shakya, E. Moon, and Z. Chang, Phys. Rev. Lett. **100**, 103906 (2008).

[5] I. J. Sola *et al.*, Nat. Phys. **2**, 319 (2006).

[6] K. T. Kim, C. Zhang, T. Ruchon, J. F. Hergott, T. Auguste, D. M. Villeneuve, P. B. Corkum, and F. Quéré, Nat. Photon. **7**, 651 (2013).

[7] T. Popmintchev *et al.*, Science **336**, 1287 (2012).

[8] M. C. Chen *et al.*, Proc. Natl. Acad. Sci. USA **111**, E2361 (2014).

[9] N. Ishii, K. Kaneshima, K. Kitano, T. Kanai, S. Watanabe, and J. Itatani, Nat. Commun. **5**, 3331 (2014).

[10] S. L. Cousin, F. Silva, S. Teichmann, M. Hemmer, B. Buades, and J. Biegert, Opt. Lett. **39**, 5383 (2014).

[11] C. Ding, W. Xiong, T. Fan, D. D. Hickstein, T. Popmintchev, X. Zhang, M. Walls, M. M. Murnane, and H. C. Kapteyn, Opt. Exp. **22**, 6194 (2014).

[12] K. Hong, C. Lai, J. P. Siqueira, P. Krogen, J. Moses, C. Chang, G. J. Stein, L. E. Zapata, and F. X. Kärtner, Opt. Lett. **39**, 3145 (2014).

[13] F. Silva, S. M. Teichmann, S. L. Cousin, M. Hemmer, and J. Biegert, Nat. Commun. **6**, 6611 (2015).

[14] J. Li, X. Ren, Y. Yin, Y. Cheng, E. Cunningham, Y. Wu, and Z. Chang, Appl. Phys. Lett. **108**, 231102 (2016).

[15] S. Hädrich, J. Rothhardt, M. Krebs, S. Demmler, A. Klenke, A. Tünnermann, and J. Limpert, J. Phys. B: At. Mol. Opt. Phys. **47**, 172002 (2016).

[16] J. Tate, T. Auguste, H. G. Muller, P. Salières, P. Agostini, and L. F. DiMauro, Phys. Rev. Lett. **98**, 013901 (2007).

[17] Y. Mairesse *et al.*, Science **302**, 1540 (2003).

[18] K. Zhao, Q. Zhang, M. Chini, Y. Wu, X. Wang, and Z. Chang, Opt. Lett. **37**, 3891 (2012).

[19] Y. Mairesse and F. Quéré, Phys. Rev. A **71**, 011401 (2005).

[20] J. Gagnon, E. Goulielmakis, and V. S. Yakovlev, Appl. Phys. B **92**, 25 (2008).

[21] V. S. Yakovlev, J. Gagnon, N. Karpowicz, and F. Krausz, Phys. Rev. Lett. **105**, 073001 (2010).

[22] H. Bachau, E. Cormier, P. Decleva, J. E. Hansen, and F. Martín, Rep. Prog. Phys. **64** 1815 (2001).

[23] O. Pronin *et al.*, Nat. Commun. **6**, 6988 (2015).

[24] M. Th. Hassan *et al.*, Nature (London) **530**, 66 (2016).

[25] C. Lu, Y. Tsou, H. Chen, B. Chen, Y. Cheng, S. Yang, M. Chen, C. Hsu, and A. H. Kung, Optica, **6**, 400 (2014).

[26] M. Chini, S. Gilbertson, S. D. Khan, and Z. Chang, Opt. Exp. **18**, 13006 (2010).

[27] H. Wei, A. T. Le, T. Morishita, C. Yu, and C. D. Lin, Phys. Rev. A **91**, 023407 (2015).

[28] P. D. Keathley, S. Bhardwaj, J. Moses, G. Laurent, and F. X. Kärtner, New J. Phys. **18**, 073009 (2016).

[29] H. Wei, T. Morishita, and C. D. Lin, Phys. Rev. A, **93** 053412 (2016).

[30] R. Pazourek, S. Nagele, and J. Burgdörfer, Rev. Mod. Phys. **87**, 765 (2015).

[31] X. M. Tong and C. D. Lin, J. Phys. B: At. Mol. Opt. Phys. **38**, 2593 (2005).